

# Is the Reaction Rate Coefficient for $\text{OH} + \text{HO}_2 \rightarrow \text{H}_2\text{O} + \text{O}_2$ Dependent on Water Vapor?

William H. Brune\* and Jena M. Jenkins

Cite This: *JACS Au* 2024, 4, 4921–4926

Read Online

ACCESS |



Metrics &amp; More



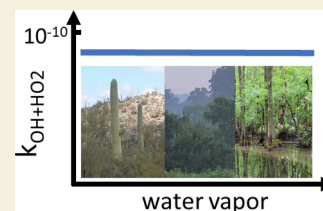
Article Recommendations



Supporting Information

**ABSTRACT:** A critical reaction affecting the oxidation chemistry in the middle-to-upper atmosphere occurs between hydroxyl (OH) and hydroperoxyl ( $\text{HO}_2$ ). The reaction rate coefficient for  $\text{OH} + \text{HO}_2 \rightarrow \text{H}_2\text{O} + \text{O}_2$ , here called  $k_{\text{OH}+\text{HO}_2}$ , has challenged laboratory kineticists for 50 years. However, several measurements from the past 30 years had approached a rough consensus until the publication of a new study that examined, for the first time, the water vapor dependence of this reaction. According to the study,  $k_{\text{OH}+\text{HO}_2}$  is not the recommended value of  $11.0 \times 10^{-11} \text{ cm}^3 \text{ molecule}^{-1} \text{ s}^{-1}$ , but instead, a water-dependent ( $\sim 1 \times 10^{-11} + 2.17 \times 10^{-28} [\text{H}_2\text{O}]$ )  $\text{cm}^3 \text{ molecule}^{-1} \text{ s}^{-1}$ . Our study examines the water dependence of  $k_{\text{OH}+\text{HO}_2}$  using water vapor photolysis of moist air at atmospheric pressure in a flow tube, with direct detection of both OH and  $\text{HO}_2$ . The observed OH decays were due only to the OH reaction with  $\text{HO}_2$  and, to a lesser extent, the OH loss to the flow tube wall and trace impurities. The resulting  $k_{\text{OH}+\text{HO}_2}$  is  $(8.54 \pm 2.90) \times 10^{-11} \text{ cm}^3 \text{ molecule}^{-1} \text{ s}^{-1}$ , 68% confidence, independent of water vapor and lower than but consistent with the recommended value.

**KEYWORDS:** hydroxyl, hydroperoxyl, reaction rate coefficient



## 1. INTRODUCTION

The atmosphere's primary oxidant, the hydroxyl radical (OH), comes from solar radiation dissociating ozone ( $\text{O}_3$ ) into molecular oxygen ( $\text{O}_2$ ) and excited-state O ( $\text{O}(^1\text{D})$ ), which then reacts with water vapor ( $\text{H}_2\text{O}$ ) to produce 2 OH molecules. OH then reacts with hundreds of chemical species, often producing a hydroperoxyl radical ( $\text{HO}_2$ ).  $\text{HO}_2$  reacts with nitric oxide (NO) or  $\text{O}_3$ , producing OH. Because the reactions lead to rapid cycling between OH and  $\text{HO}_2$ , the sum of them,  $\text{OH} + \text{HO}_2$ , is often called  $\text{HO}_x$ . This cycling continues until  $\text{HO}_2$  or OH termination reactions form more stable chemical species. One of the most important termination reactions is reaction:



This reaction terminates both OH and  $\text{HO}_2$ , returning the radicals to water vapor.

This reaction influences atmospheric chemistry in several ways. First, throughout most of the troposphere, away from urban areas and other large NO sources, this reaction removes from the troposphere a sizable amount of  $\text{HO}_x$ , about 15% near Earth's surface, growing to  $\sim 50\%$  above 10 km altitude.<sup>1</sup> Second, extreme amounts of OH and  $\text{HO}_2$  were recently found to be produced directly by lightning and weaker electrical discharges in thunderstorm outflow anvil clouds.<sup>2</sup> This lightning-generated OH, called LOH, is calculated to be responsible for 2–16% of global OH oxidation, but this calculation depends heavily on the reaction rate coefficient of  $\text{OH} + \text{HO}_2 \rightarrow \text{H}_2\text{O} + \text{O}_2$ , here called  $k_{\text{OH}+\text{HO}_2}$ . This reaction removes over half of the OH before it can react with carbon

monoxide (CO) or other chemical species. Thus, the value of the reaction rate coefficient is critical for determining the atmosphere's oxidation capacity and thus lifetimes of CO, methane ( $\text{CH}_4$ ), and other atmospheric constituents.

The value of the IUPAC recommended reaction rate coefficient in Atkinson et al.<sup>3</sup> for the reaction of  $\text{OH} + \text{HO}_2 \rightarrow \text{H}_2\text{O} + \text{O}_2$  is

$$k_{\text{OH}+\text{HO}_2}^{\text{IUPAC}} = 4.8 \times 10^{-11} \exp(250/T) \text{ cm}^3 \text{ molecule}^{-1} \text{ s}^{-1}$$

where  $T$  is temperature. At  $T = 298 \text{ K}$ ,  $k_{\text{OH}+\text{HO}_2}^{\text{IUPAC}} = 11.0 \times 10^{-11} \text{ cm}^3 \text{ molecule}^{-1} \text{ s}^{-1}$ . This recommendation is based on six studies that measured OH and in some cases also  $\text{HO}_2$ .<sup>4–9</sup>

Two early studies that estimated  $\text{OH} + \text{HO}_2 \rightarrow \text{H}_2\text{O} + \text{O}_2$  by looking at the effects of secondary chemistry on the reactions of OH with either hydrogen peroxide ( $\text{H}_2\text{O}_2$ ) or ozone ( $\text{O}_3$ ) found rate coefficients of  $(1–3) \times 10^{-11} \text{ cm}^3 \text{ molecule}^{-1} \text{ s}^{-1}$ .<sup>10,11</sup> A 2020 study by Assaf and Fittschen<sup>12</sup> using direct measurements of OH and  $\text{HO}_2$  measured  $10.2 \times 10^{-11} \text{ cm}^3 \text{ molecule}^{-1} \text{ s}^{-1}$ , consistent with the IUPAC recommendation. None of these studies examined the reaction rate coefficient as a function of water vapor over a substantial range.

A 2023 study did. Speak et al.<sup>13</sup> used two different laboratory systems and theoretical calculations to study

**Received:** September 26, 2024

**Revised:** November 14, 2024

**Accepted:** November 15, 2024

**Published:** November 22, 2024



Table 1. Characteristics of Laboratory Setup and Experiments

| component                | characteristics   | uncertainty (68% confidence) |
|--------------------------|---|------------------------------|
| flow tube                | material: fused quartz; I.D.: 4.6 cm; length: 105 cm  |                              |
| flow amount              | flow: 50 LPM; pressure: 950–1000 hPa; $T = 294$ K; $R_e \sim 1500$ ; measured centerline velocity: $86 \text{ cm s}^{-1}$ ; radial flow profile: not quite fully developed laminar flow   | <5%                          |
| stable gases             | air (dewpoint: $-40$ °C; $\text{CO} \sim 20$ ppbv; OH reactivity $<0.5 \text{ s}^{-1}$ ); HPLC-grade water (400–15,000 ppmv)  | N/A                          |
| detection                | OH: LIF in 6 hPa detection cell, sampled through 1 mm hole perpendicular to flow and 0.5 cm from flow tube centerline   | $\pm 20\%$                   |
|                          | $\text{HO}_2$ : $\text{NO} + \text{HO}_2 \rightarrow \text{OH} + \text{NO}_2$ , OH LIF in detection cell  | $\pm 20\%$                   |
|                          | $\text{O}_3$ : UV absorption, Thermo 49C  | $\pm 5\%$                    |
|                          | $\text{H}_2\text{O}$ , pressure, temperature: Vaisala HMT310  | $\pm 5\%$                    |
| signals                  | OH signal: online $5\text{--}500 \text{ cts s}^{-1}$ ; off-line $0.2 \text{ cts s}^{-1}$  |                              |
|                          | $\text{HO}_2$ signal: online $20\text{--}2000 \text{ cts s}^{-1}$ ; off-line $0.2 \text{ cts s}^{-1}$   |                              |
| OH/ $\text{HO}_2$ source | UV Hg lamp (Atlantic Ultraviolet 16007-V177); placed $0.5 \text{ cm}$ above quartz flow tube; $185:254 \text{ nm} < 0.1$ ; $8 \text{ mm}$ slit perpendicular to flow; $\text{flux}_{254 \text{ nm}} < 10^{15} \text{ photons cm}^{-2} \text{ s}^{-1}$ <sup>16</sup> |                              |
|                          | UV varied by covering with FEP sheets ( $0.12 \text{ mm}$ thick)  |                              |
| OH decays                | five $5 \text{ cm}$ steps between $15\text{--}35 \text{ cm}$ from $\text{HO}_x$ sampling inlet; OH decay found by least-squares fit to $\log(\text{OH})$ versus reaction time for each experiment   | $\pm 20\%$                   |
| wall loss and impurities | OH: $0.9 \text{ s}^{-1}$ ; impurity: $0.35 \text{ s}^{-1}$ ; total: $1.25 \text{ s}^{-1}$   | $\pm 0.3 \text{ s}^{-1}$     |
|                          | $\text{HO}_2$ : $<0.3 \text{ s}^{-1}$   |                              |
| initial radical ranges   | OH: $3.5 \times 10^9\text{--}2.6 \times 10^{10} \text{ cm}^{-3}$  |                              |
|                          | $\text{HO}_2$ : $7.2 \times 10^9\text{--}1.0 \times 10^{11} \text{ cm}^{-3}$  |                              |
|                          | $\text{O}_3$ : $0\text{--}70$ ppbv, except 3 experiments at $\sim 120$ ppbv   |                              |
| number of experiments    | OH wall loss: 22  |                              |
|                          | OH + $\text{HO}_2$ rate coefficient: 51   |                              |

$k_{\text{OH}+\text{HO}_2}$  and its water dependence. They determined the  $k_{\text{OH}+\text{HO}_2}$  to be  $\sim 1 \times 10^{-11} \text{ cm}^3 \text{ molecule}^{-1} \text{ s}^{-1}$  when water vapor was  $\sim 10^{16} \text{ cm}^{-3}$ , increasing to  $8 \times 10^{-11} \text{ cm}^3 \text{ molecule}^{-1} \text{ s}^{-1}$  when water vapor was greater than  $3 \times 10^{17} \text{ cm}^{-3}$ . The water vapor dependence was determined to be  $2.17 \times 10^{-28} \text{ cm}^6 \text{ molecule}^{-1} \text{ s}^{-1}$ . If this result is correct, then OH in the upper troposphere and the impact of lightning-produced OH on global OH oxidation must be reassessed.

In response to the Speak et al.<sup>13</sup> results, Chen et al.<sup>14</sup> used the same method as Assaf and Fittchen<sup>12</sup> for determining  $k_{\text{OH}+\text{HO}_2}$ , but this time, the experiments were performed with either no added water vapor or  $[\text{H}_2\text{O}] = 6.32 \times 10^{16} \text{ cm}^{-3}$ . In both cases, they obtained  $k_{\text{OH}+\text{HO}_2} = (11.0 \pm 0.12) \times 10^{-11} \text{ cm}^3 \text{ molecule}^{-1} \text{ s}^{-1}$ , indicating that  $k_{\text{OH}+\text{HO}_2}$  is independent of water vapor.

In this study, we examine the reaction rate coefficient for  $\text{OH} + \text{HO}_2 \rightarrow \text{H}_2\text{O} + \text{O}_2$  and its water vapor dependence over a range of water vapor concentrations using the simplest, near-atmospheric-like chemistry we could imagine. It involves flowing mixtures of atmospheric pressure air and water vapor past a moveable ultraviolet radiation source and detecting both OH and  $\text{HO}_2$  at the end of the flow tube. By varying the water vapor concentrations and  $\text{HO}_x$  production and directly measuring the OH and  $\text{HO}_2$  decays, we were able to determine the  $k_{\text{OH}+\text{HO}_2}$  and its water vapor dependence. We compare and contrast our results with those of the previously mentioned references.

## 2. EXPERIMENTAL DESIGN AND EXECUTION

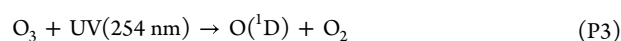
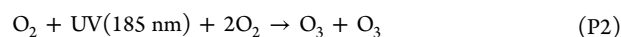
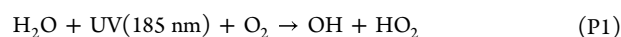
Our experiments use the discharge-flow method for measuring the decay of OH in the presence of excess  $\text{HO}_2$ . Details of this apparatus can be found in Jenkins et al.<sup>15</sup> Relevant details for this study are listed in Table 1. The experimental apparatus consists of a flow tube used primarily for research on OH,  $\text{HO}_2$ , NO,  $\text{NO}_2$ ,  $\text{O}_3$ , and other products of electrical discharges including sparks and corona. However, instead of a fixed discharge to create OH and a moveable one for  $\text{HO}_2$  as has been used before,<sup>7</sup> a moveable mercury (Hg) lamp, positioned just above the quartz flow tube, emits both the 185

and 254 nm radiation to create both OH and  $\text{HO}_2$  in a disc filling the flow tube cross section and  $\sim 1 \text{ cm}$  thick along the tube length. Less than 20% of the 185 nm radiation is absorbed even at the tube bottom, resulting in a fairly uniform distribution of OH and  $\text{HO}_2$  throughout the tube's cross-section. Both OH and  $\text{HO}_2$  were measured by the Ground-based Hydrogen Oxides Sensor (GTHOS), with its inlet sampling from the center of the flow at the end of the flow tube.<sup>15,17</sup>

GTHOS measures OH by laser-induced fluorescence (LIF) in air that was pulled through a 1 mm pinhole past two detection chambers at 6 hPa pressure. OH absorbs the laser radiation in the  $Q_1(2)$  line at 307.9948 nm (called online) and its fluorescence was detected by a gated microchannel plate set at right angles to the laser beam and the flow. The laser was pulsed at 3 kHz, has an average power of 0.5–7 mW, and was passed through the airflow 32 times with a multipass cell. For this experiment, the laser power was  $\sim 1 \text{ mW}$  and the beam diameter at the center of the detection cell was  $\sim 4 \text{ mm}$ . To distinguish the OH fluorescence signal from background signals, 25 s of online were followed by 5 s of offline, with the laser wavelength shifted, alternately,  $-0.008$  or  $+0.008 \text{ nm}$  from the online wavelength.  $\text{HO}_2$  is detected when NO is added upstream of the detection cell and reacts with  $\text{HO}_2$  to produce OH, which is detected by LIF.

For each experiment, OH and  $\text{HO}_2$  were measured as the UV lamp was moved further away from the GTHOS inlet in five steps, collecting signal for 30 s at each step. A linear least-squares fit to the logarithm of these OH data as a function of the reaction time gave a slope equal to the OH decay ( $\text{s}^{-1}$ ).

In the flow tube, the stable gas composition is  $\text{N}_2$ ,  $\text{O}_2$ , and  $\text{H}_2\text{O}$ . Photolysis by the UV lamp initiates fairly simple chemistry, as shown in the following reaction sequence, where “P” indicates  $\text{HO}_x$  production and “R” indicates OH reactions.





No reactions with  $\text{H}_2\text{O}_2$  as a reactant are listed because only small amounts of  $\text{H}_2\text{O}_2$  would be produced and the modeled  $\text{H}_2\text{O}_2$  for these conditions does not exceed  $5 \times 10^9 \text{ cm}^{-3}$ . Thus, the  $\text{OH} + \text{H}_2\text{O}_2$  reaction frequency, with a rate coefficient of  $k_{\text{OH}+\text{H}_2\text{O}_2} = 1.7 \times 10^{-12} \text{ cm}^3 \text{ molecules}^{-1} \text{ s}^{-1}$ , is negligible. With  $\text{O}_3$  less than 70 ppbv ( $1.7 \times 10^{12} \text{ cm}^{-3}$ ), R2 and R3 affect the OH decays by less than 4%, although their contributions are still subtracted from the calculated decay slopes of individual experiments. More than 95% of each OH decay is due to R1 and R4.

The frequency for R4 is half the total OH decay for  $[\text{HO}_2]_{\text{initial}} < 2 \times 10^{10} \text{ cm}^{-3}$ , but shrinks to less than 20% for  $[\text{HO}_2]_{\text{initial}} > 5 \times 10^{10} \text{ cm}^{-3}$ . Thus, the frequency for R4 is a large enough fraction that it must be quantified and subtracted from the calculated OH decay slope. To measure this frequency, we decreased  $\text{HO}_2$  and OH by reducing water vapor and/or UV flux. The lower  $\text{HO}_2$  reduced the contributions of R1, R2, and R3 to the OH decays while maintaining enough OH to measure the OH decay slope.

In these measurements, the contribution of R1 to the OH wall decay slope varied from 10 to 35% if the IUPAC reaction rate coefficient was used. (Note: in the Discussion, we describe the impact of using the reaction rate coefficient from Speak et al.<sup>13</sup> in this analysis.) Once  $k_{\text{OH}+\text{HO}_2}$  was found, it was used to correct the wall loss frequency, which was then used to find an updated value of  $k_{\text{OH}+\text{HO}_2}$ . The updated  $k_{\text{OH}+\text{HO}_2}$  was then used to find a new value for the wall loss frequency. In the second iteration, the new wall loss frequency was less than 1% different from the previous value, so the iterations were stopped, and the updated  $k_{\text{OH}+\text{HO}_2}$  was adopted as the reported value. The resulting average OH wall loss/impurity frequency is  $(1.25 \pm 0.3) \text{ s}^{-1}$ , 68% confidence.

In the experiments to find the loss frequency for the wall loss and impurity,  $\text{HO}_2$  increased slightly, while OH decreased.  $\text{HO}_x$ , the sum of OH and  $\text{HO}_2$ , decreased less than OH, suggesting that some of the OH loss is due to reactions that cycle OH into  $\text{HO}_2$ . The  $\text{HO}_x$  decay will not be influenced by reactions with impurities that cycle  $\text{HO}_x$  between OH and  $\text{HO}_2$ , but it will be influenced by terminal losses of OH and  $\text{HO}_2$ . From the analysis of the  $\text{HO}_x$  decays, the loss frequency of R4 due to wall loss is  $\sim 0.9 \text{ s}^{-1}$ , leaving  $\sim 0.35 \text{ s}^{-1}$  for an impurity reacting with OH to form  $\text{HO}_2$ . The measured CO accounts for less than half of that impurity.

**Reaction P1** produces equal amounts of OH and  $\text{HO}_2$ , but in the  $\sim 0.2 \text{ s}$  between the GTHOS inlet and the first accessible measuring point, OH had dropped more than  $\text{HO}_2$  because of greater wall and impurity losses. On average, for the OH decay measurements,  $\text{HO}_2$  started 4 times larger than OH, with a range of 2–10, and dropped on average 15% during the experiment, with a range of 0–30%. Furthermore, the  $\text{HO}_2$  decrease between the first and final steps is within 15% of the OH decrease when it is corrected for wall/impurity loss. This similar decrease indicates that  $k_{\text{OH}+\text{HO}_2}$  is removing them both, as expected. Thus, although the initial loss of equal amounts of OH and  $\text{HO}_2$  by R1 is quadratic, by the time OH and  $\text{HO}_2$  are measured,  $\text{HO}_2$  is in excess. We can assume that the OH decay is pseudo-first-order using the average  $\text{HO}_2$  as the excess reactant for each experiment:

$$k_{\text{OH}+\text{HO}_2} = \frac{\text{dlog}(\text{OH})/\text{dt} - k_{\text{wall}} - k_{\text{OH}+\text{O}_3}[\text{O}_3]}{[\text{HO}_2]_{\text{average}}} \quad (\text{E1})$$

The uncertainty in the derived rate coefficient for  $k_{\text{OH}+\text{HO}_2}$  is dictated primarily by the uncertainties in the OH wall loss, the  $\text{HO}_2$  measurement, and the uncertainty due to the precision of the measured OH decays. The precision uncertainty is taken as the standard deviation of the calculated  $k_{\text{OH}+\text{HO}_2}$  and is due to variations in the calculated slopes, as discussed further in the results. Uncertainties in the reaction frequencies of  $\text{OH} + \text{O}_3$  and  $\text{OH} +$

OH are small enough to be neglected in this propagation-of-error analysis. Since the fractional uncertainty in  $k_{\text{wall}}$  is  $\pm 0.25$ , in  $[\text{HO}_2]_{\text{average}}$  is  $\pm 0.20$ , and in the OH decay slope measurement is  $\pm 0.20$ , all at 68% confidence, the resulting uncertainty in  $k_{\text{OH}+\text{HO}_2}$  is  $\pm 34\%$ , 68% confidence.

This study is the first time this laboratory flow system has been used to measure a reaction rate coefficient. Measuring reaction rate coefficients in a flow tube under these conditions (970 hPa; 86 cm  $\text{s}^{-1}$ ; 4.6 cm diameter) is uncommon. However, the measured radial velocity profile and the centerline velocity are consistent with expectations for flow approaching but not yet at fully developed laminar flow. To test this system, we chose to find the rate coefficients for two reactions: OH with  $\alpha$ -pinene and OH with perfluoropropylene for two reactions: OH with  $\alpha$ -pinene and OH with perfluoropropylene ( $\text{C}_3\text{F}_6$ ).

For the  $\alpha$ -pinene reaction, known amounts of  $\alpha$ -pinene (Aldrich, 98% pure) were added to the humidified air in the flow tube using a syringe pump (Chemyx Inc., Fusion 100) to inject  $\alpha$ -pinene into a 1 LPM flow, which was added to the main 49 LPM flow in 1/2" Teflon tubing prior to the air entering the flow tube. The flow-tube pressure was 970 hPa and the temperature was 294 K. The  $\alpha$ -pinene concentrations in nine experiments ranged from  $6.7 \times 10^{10}$  to  $2.0 \times 10^{11} \text{ cm}^{-3}$ , resulting in the range of OH reactivity from this reaction from 3.6 to  $10.8 \text{ s}^{-1}$ . Other contributors to the OH decay were OH +  $\text{HO}_2$  ( $0.8\text{--}2.9 \text{ s}^{-1}$ ) and OH wall/impurity loss ( $1.25 \text{ s}^{-1}$ ). Subtracting these additional contributors from the linear-least-squares slope to the OH decay resulted in  $k_{\text{OH}+\text{AP}} = (5.1 \pm 0.7) \times 10^{-11} \text{ cm}^3 \text{ molecule}^{-1} \text{ s}^{-1}$ , where the uncertainty is precision only. This result is consistent with the IUPAC rate coefficient of  $k_{\text{OH}+\text{AP}} = 5.4 \times 10^{-11} \text{ cm}^3 \text{ molecule}^{-1} \text{ s}^{-1}$ .<sup>3</sup>

For the  $\text{C}_3\text{F}_6$  experiments, a few hPa of  $\text{C}_3\text{F}_6$  were drawn from the gas over liquid  $\text{C}_3\text{F}_6$  (SynQuest Laboratories, 98.5% pure) into a stainless steel reservoir, to which  $\sim 2000 \text{ hPa}$  of high-purity  $\text{N}_2$  (Linde, 99.999% pure) was added. This  $\text{C}_3\text{F}_6/\text{N}_2$  mixture was flowed at rates between 0 and 5 standard cubic centimeters per minute (sccm) into total flow (50,000 sccm), resulting in five values of  $[\text{C}_3\text{F}_6]$  from 0 to  $2.2 \times 10^{12} \text{ cm}^{-3}$ . Although  $\text{C}_3\text{F}_6$  can be photolyzed by the 185 nm radiation with an absorption cross-section of  $\sim 10^{-17} \text{ cm}^2$ ,<sup>18</sup> photolysis with the UV flux given in Table 1 would produce a negligible amount ( $< 2 \text{ pptv}$ ) of a fluorine radical. Three different combinations of water vapor and UV filters were used to make different amounts of OH and  $\text{HO}_2$ . Initial OH was  $(0.4\text{--}1) \times 10^{10} \text{ cm}^{-3}$  and, for each of the combinations,  $\text{HO}_2$  was independent of  $\text{C}_3\text{F}_6$  and  $(1\text{--}2) \times 10^{10} \text{ cm}^{-3}$ . The slope of the OH decay rate versus  $[\text{C}_3\text{F}_6]$  for all 16 experiments gave a reaction rate coefficient of  $(2.10 \pm 0.30) \times 10^{-12} \text{ cm}^3 \text{ molecule}^{-1} \text{ s}^{-1}$  and the mean of all values with  $[\text{C}_3\text{F}_6] > 0$  is  $(2.24 \pm 0.39) \times 10^{-12} \text{ cm}^3 \text{ molecule}^{-1} \text{ s}^{-1}$ . This result is consistent with the IUPAC recommendation of  $2.18 \times 10^{-12} \text{ cm}^3 \text{ molecule}^{-1} \text{ s}^{-1}$ .<sup>3</sup> Our measured rate coefficients for OH with  $\alpha$ -pinene and with perfluoropropylene demonstrate that this laboratory flow system is suitable for measuring OH reaction rate coefficients.

For  $\text{OH} + \text{HO}_2 \rightarrow \text{H}_2\text{O} + \text{O}_2$ , some OH decays were calculated with a photochemical box model to ensure that the approximations leading to E1 were valid. The MCMv3.3.1 mechanism<sup>19</sup> was run using the F0AM photochemical box modeling framework.<sup>20</sup> The inputs to the model included the measured values for pressure, temperature,  $\text{H}_2\text{O}$ ,  $\text{O}_3$ , CO, OH wall loss frequency, initial OH, initial  $\text{HO}_2$ , and calculated  $k_{\text{OH}+\text{HO}_2}$ . The model was run for 0.25 s and the intermediate steps were saved.

### 3. RESULTS

We calculated  $k_{\text{OH}+\text{HO}_2}$  for each of the fifty-one OH decays. Four typical OH decays out of the fifty-one experiments are shown in Figure 1. The measurements are the markers, the linear least-squares fits are the colored lines, and the model-calculated OH decays are the gray dashed lines. For these four experiments, the initial OH ranged from  $0.7 \times 10^{10}$  to  $1.3 \times 10^{10} \text{ cm}^{-3}$ , but each one has been scaled to the mean value of the four initial points so that the decays from the different



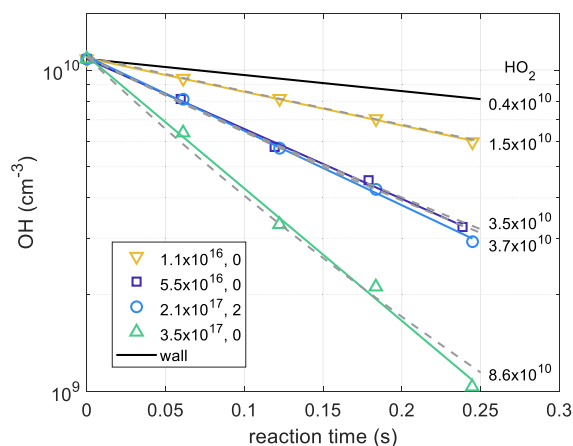


**Figure 1.** OH decays vs reaction time. Five OH typical decays, including wall loss, are shown along with their average HO<sub>2</sub> concentrations. Initial OH values have been scaled to the mean initial value for the plot. The legend shows the water vapor concentration and the number of UV filters used for each experiment. Gray dashed lines show the scaled OH decays as calculated with the MCMv3.3.1 model.

experiments can be more easily compared. To the right of the decays are the average HO<sub>2</sub> concentrations for each experiment. The OH decreases from less than a factor of 2 to a factor of 10. The legend gives the water vapor concentration and number of filters used for each experiment.

Note the middle two OH decays that are almost identical, as are their average HO<sub>2</sub> concentrations. For the OH decay with HO<sub>2</sub> = 3.5 × 10<sup>10</sup> cm<sup>-3</sup>, this HO<sub>2</sub> was achieved using 5.5 × 10<sup>16</sup> cm<sup>-3</sup> of water vapor and no filters, while the OH decay with HO<sub>2</sub> = 3.7 × 10<sup>10</sup> cm<sup>-3</sup> was achieved with 2.1 × 10<sup>17</sup> cm<sup>-3</sup> of water vapor and 2 UV filters reducing the 185 nm radiation. The similarity in these two decays despite the factor-of-four difference in water vapor indicates that *k*<sub>OH+HO<sub>2</sub></sub> is independent of water vapor.

The reaction frequencies for OH + HO<sub>2</sub> → H<sub>2</sub>O + O<sub>2</sub>, the combined reactions of OH with O<sub>3</sub> and OH, and the OH wall loss are shown for the 51 experiments in Figure 2. The experiments are arranged from the lowest water vapor to the highest. The scatter in *k*<sub>OH+HO<sub>2</sub></sub> appears to be independent of

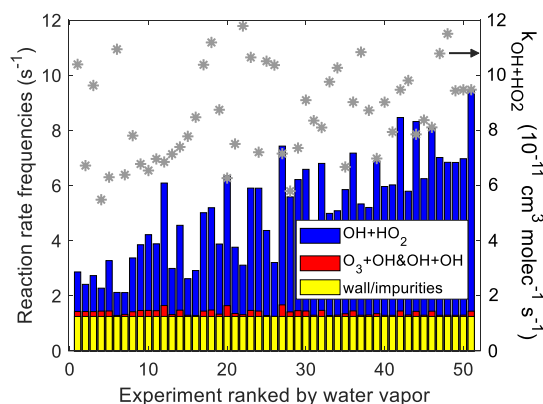


**Figure 2.** Reaction rate frequencies for the 51 experiments ordered by water vapor. Left axis: reaction frequencies for OH + HO<sub>2</sub> (blue), O<sub>3</sub> + OH + OH (red), and wall and impurities (yellow) are shown as bars. Right axis: *k*<sub>OH+HO<sub>2</sub></sub> for the 51 experiments are given as gray stars.

water vapor, the reaction frequency of OH + HO<sub>2</sub> → H<sub>2</sub>O + O<sub>2</sub>, and the difference between the reaction frequency of OH + HO<sub>2</sub> → H<sub>2</sub>O + O<sub>2</sub> and the OH wall loss frequency. Thus, the scatter in *k*<sub>OH+HO<sub>2</sub></sub> is due to other factors, especially statistical variation.

The reaction rate coefficient *k*<sub>OH+HO<sub>2</sub></sub> for the 51 experiments is shown in Figure 3. The 51 individual experiments (gray

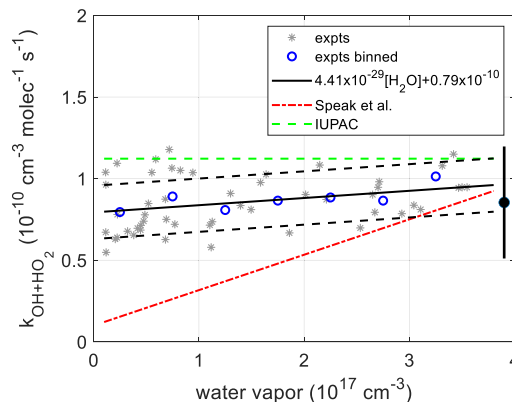


**Figure 3.** OH + HO<sub>2</sub> reaction rate coefficient as a function of water vapor. Shown are the *k*<sub>OH+HO<sub>2</sub></sub> of all 51 individual experiments (gray stars); the *k*<sub>OH+HO<sub>2</sub></sub> averaged into 0.5 × 10<sup>17</sup> cm<sup>-3</sup> bins (blue circles); the linear fit to experiments (black line); the standard deviation in *k*<sub>OH+HO<sub>2</sub></sub> at 68% confidence (dashed black lines); the IUPAC recommendation (green dashed line); and the Speak et al.<sup>13</sup> water-dependent *k*<sub>OH+HO<sub>2</sub></sub> (red dash-dot line). Average *k*<sub>OH+HO<sub>2</sub></sub> and its total error (68% confidence) are shown to the right (black dot and lines) and is (8.54 ± 2.90) × 10<sup>-11</sup> cm<sup>3</sup> molecule<sup>-1</sup> s<sup>-1</sup>.

stars) are distributed over the water vapor range, but because the focus of this study was to test the Speak et al.<sup>13</sup> results, half the experiments were conducted at lower water vapor concentrations and thus they have smaller decay slopes and greater statistical variability. Also shown in the figure are *k*<sub>OH+HO<sub>2</sub></sub> averaged for water vapor bins of 5 × 10<sup>16</sup> cm<sup>-3</sup>, the linear least-squares fit to the 51 experimental results in the solid black line, along with its uncertainty at 68% confidence, and dashed lines for *k*<sub>OH+HO<sub>2</sub></sub> from IUPAC<sup>3</sup> and Speak et al.<sup>13</sup>

#### 4. DISCUSSION

This study has some differences from previous studies. First, in this study, all experiments were conducted in air at atmospheric pressure, while most other studies used N<sub>2</sub>, Ar, or He as the carrier gas, usually at a lower-than-atmospheric pressure. Second, the reaction frequency range used in this study was ~3–10 s<sup>-1</sup>, while all other studies had reaction frequency ranges 10–100 times larger. Third, the chemistry in this study was designed to minimize all chemical reactions except the reaction of OH + HO<sub>2</sub>, with the OH wall loss/impurity as the only competition. Fourth, only Speak et al.<sup>13</sup> and this study examine the dependence of *k*<sub>OH+HO<sub>2</sub></sub> on water vapor over the atmospherically relevant range from ~10<sup>16</sup> to ~3 × 10<sup>17</sup> cm<sup>-3</sup>.

As shown in Figure 3, the linear least-squares fit to our experiments has a water vapor dependence of 4.4 × 10<sup>-29</sup> cm<sup>6</sup> molecule<sup>-1</sup> s<sup>-1</sup>, although the slope is not statistically significant. If we assume the slope is real and the water vapor dependence is due to the formation of the HO<sub>2</sub>–H<sub>2</sub>O complex using the equilibrium constant given in the study of Speak et al.,<sup>15</sup> then the reaction of OH with the complex would

need a reaction rate coefficient of  $\sim 8 \times 10^{-11} \text{ cm}^3 \text{ molecule}^{-1} \text{ s}^{-1}$ , nearly identical to the water independent intercept for  $k_{\text{OH}+\text{HO}_2}$ . Further, the close similarity of the two middle OH decays in Figure 1, despite the factor-of-four difference in water vapor, provides additional evidence that  $k_{\text{OH}+\text{HO}_2}$  calculated from our 51 experiments is independent of water vapor. If Speak et al.<sup>13</sup> were correct, the slopes of these two decays would be different by a factor of 2.5. Thus, our results support a water-independent  $k_{\text{OH}+\text{HO}_2}$  at 68% confidence, of  $(8.54 \pm 2.90) \times 10^{-11} \text{ cm}^3 \text{ molecule}^{-1} \text{ s}^{-1}$ .

As mentioned in the Experiment design and execution section, the values for OH wall loss are somewhat dependent on the  $k_{\text{OH}+\text{HO}_2}$  used to correct the wall loss decays. If the Speak et al.<sup>13</sup> value is used, then the calculated wall loss frequency becomes  $1.5 \text{ s}^{-1}$ . When this value is used to calculate  $k_{\text{OH}+\text{HO}_2}$  from our data as a function of water vapor,  $k_{\text{OH}+\text{HO}_2} = 7.4 \times 10^{-29} [\text{H}_2\text{O}] + 0.67 \times 10^{-10} \text{ cm}^3 \text{ molecule}^{-1} \text{ s}^{-1}$ . As before this water vapor dependence is statistically insignificant and the averaged  $k_{\text{OH}+\text{HO}_2}$  is  $(7.75 \pm 2.64) \times 10^{-11} \text{ cm}^3 \text{ molecule}^{-1} \text{ s}^{-1}$ , which is 14% lower than the  $k_{\text{OH}+\text{HO}_2}$  we found from these experiments using the IUPAC<sup>3</sup>  $k_{\text{OH}+\text{HO}_2}$  to correct the wall loss and 10% lower than the  $k_{\text{OH}+\text{HO}_2}$  we found from these experiments using our  $k_{\text{OH}+\text{HO}_2}$  to correct the wall loss.

The  $k_{\text{OH}+\text{HO}_2}$  from our experiments is lower than but consistent with the IUPAC recommendation and the several studies that support that recommendation<sup>3–9</sup> as well as the more recent studies by Assaf and Fittschen<sup>12</sup> and Chen et al.<sup>14</sup> At water vapor concentrations less than  $\sim 2 \times 10^{17} \text{ cm}^{-3}$ , our result is inconsistent with the water-dependent result of Speak et al.<sup>13</sup> We have no definitive explanation for this substantial difference with Speak et al.,<sup>13</sup> especially for their theoretical water-dependent result.

The 2016–2018 NASA Atmospheric Tomography (ATom) study was a series of aircraft flights south over the central Pacific Ocean, east over Antarctica, north over in Atlantic Ocean, and west over northern Canada, once in each Northern Hemisphere season. These flights consisted of almost constant ascents to 10–14 km followed by descents to  $\sim 0.2 \text{ km}$ , thus scanning almost the entire troposphere. The airborne configuration of GTHOS, called ATHOS, was on these flights.<sup>1</sup> At altitudes above 4 km, water vapor was less than  $10^{17} \text{ cm}^{-3}$ , and according to Speak et al.,<sup>13</sup>  $k_{\text{OH}+\text{HO}_2}$  should be less than  $3 \times 10^{-11} \text{ cm}^3 \text{ molecule}^{-1} \text{ s}^{-1}$ . On average for altitudes above 4 km and different latitude bands, the percent difference  $(100 \times \frac{\text{observation} - \text{model}}{(\text{observation} + \text{model}) / 2})$  for OH is less than 30% and for  $\text{HO}_2$  is less than 20% for the model using the IUPAC<sup>3</sup> recommendation for  $k_{\text{OH}+\text{HO}_2}$ . If the Speak et al.<sup>13</sup> value is used instead, the percent difference is less than that using the IUPAC<sup>3</sup> by as much as 10–15% at some altitudes and latitudes and a similar amount larger for other altitudes and latitudes. In all cases, the percent differences using either Speak et al.<sup>13</sup> or IUPAC<sup>3</sup> are within the combined model and observation uncertainty of  $\sim \pm 40\%$ . Thus, the ATom results provide no evidence for or against the  $k_{\text{OH}+\text{HO}_2}$  from Speak et al.<sup>13</sup>

## 5. CONCLUSIONS

Speak et al.<sup>13</sup> raised an interesting question about the water vapor dependence of the reaction between OH and  $\text{HO}_2$ . Using our laboratory system designed for electrical discharge studies, we devised flow-tube experiments that measure OH and  $\text{HO}_2$  directly in the simplest chemistry we could conceive

at atmospherically relevant gas compositions and pressure. In the final analysis, these experiments provide substantial evidence that  $\text{OH} + \text{HO}_2 \rightarrow \text{H}_2\text{O} + \text{O}_2$  is independent of water vapor and has a room temperature rate coefficient of  $(8.54 \pm 2.90) \times 10^{-11} \text{ cm}^3 \text{ molecule}^{-1} \text{ s}^{-1}$ , 68% confidence, lower than but consistent with current IUPAC recommendations.<sup>3</sup> While our result is consistent with the IUPAC recommendation,<sup>3</sup> it is  $\sim 30\%$  lower and would result in OH being  $\sim 5\%$  greater in the upper troposphere and in thunderstorms. We recommend the use of a water-vapor-independent reaction rate coefficient and the re-evaluation of the IUPAC recommendation considering this new lower  $k_{\text{OH}+\text{HO}_2}$ .

## ■ ASSOCIATED CONTENT

### Supporting Information

The Supporting Information is available free of charge at <https://pubs.acs.org/doi/10.1021/jacsau.4c00905>.

Experimental data used to determine the  $\text{OH} + \text{HO}_2 \rightarrow \text{H}_2\text{O} + \text{O}_2$  reaction rate coefficient; variables are experiment number, and, for each experiment, pressure, temperature, number concentration, time step for the five OH measurements in each decay,  $\text{H}_2\text{O}$  concentration, number of UV filters,  $\text{O}_3$  concentration,  $\text{HO}_2$  concentration averaged over the OH decay for each experiment, and OH concentration for each of the five lamp positions in 5 cm increments (PDF)

## ■ AUTHOR INFORMATION

### Corresponding Author

William H. Brune – Department of Meteorology and Atmospheric Science, Pennsylvania State University, University Park, Pennsylvania 16802, United States; [orcid.org/0000-0002-1609-4051](https://orcid.org/0000-0002-1609-4051); Email: [whb2@psu.edu](mailto:whb2@psu.edu)

### Author

Jena M. Jenkins – Department of Meteorology and Atmospheric Science, Pennsylvania State University, University Park, Pennsylvania 16802, United States

Complete contact information is available at: <https://pubs.acs.org/doi/10.1021/jacsau.4c00905>

### Author Contributions

CRediT: William H. Brune conceptualization, formal analysis, investigation, visualization, writing - original draft, writing - review & editing; Jena M Jenkins investigation, writing - review & editing.

### Funding

This study was supported by NSF grant AGS-2323203 and NASA grant 80NSSC19K1590.

### Notes

The authors declare no competing financial interest.

## ■ ACKNOWLEDGMENTS

We thank Y. Yung for calling our attention to Speak et al.,<sup>13</sup> P. Stevens for lending us a microchannel plate detector after ours failed, and two anonymous reviewers for their comments.

## REFERENCES

- (1) Brune, W. H.; Miller, D. O.; Thames, A. B.; Allen, H. M.; Apel, E. C.; Blake, D. R.; Bui, T. P.; Commane, R.; Crounse, J. D.; Daube, B. C.; et al. Exploring Oxidation in the Remote Free Troposphere: Insights From Atmospheric Tomography (ATom). *J. Geophys. Res.: Atmos.* **2020**, *125*, No. e2019JD031685.
- (2) Brune, W. H.; McFarland, P. J.; Bruning, E.; Waugh, S.; MacGorman, D.; Miller, D. O.; Jenkins, J. M.; Ren, X.; Mao, J.; Peischl, J. Extreme oxidant amounts produced by lightning in storm clouds. *Science* **2021**, *372*, 711–715.
- (3) Atkinson, R.; Baulch, D. L.; Cox, R. A.; Crowley, J. N.; Hampson, R. F.; Hynes, R. G.; Jenkin, M. E.; Rossi, M. J.; Troe, J. Evaluated kinetic and photochemical data for atmospheric chemistry: Volume I - gas phase reactions of O<sub>x</sub>, HO<sub>x</sub>, NO<sub>x</sub> and SO<sub>x</sub> species. *Atmos. Chem. Phys.* **2004**, *4*, 1461–1738.
- (4) Braun, M.; Hofzumahaus, A.; Stuhl, F. VUV Flash Photolysis Study of the Reaction of HO with HO<sub>2</sub> at 1 atm and 298 K. *Berichte der Bunsengesellschaft für physikalische Chemie* **1982**, *86*, 597–602.
- (5) Dransfeld, P.; Wagner, H. G. Comparative Study of the Reactions of <sup>16</sup>OH and <sup>18</sup>OH with H<sup>16</sup>O<sub>2</sub>. *Z. Naturforsch., A: Phys. Sci.* **1987**, *42* (5), 471–476.
- (6) Keyser, L. F. Kinetics of the reaction OH + HO<sub>2</sub> → H<sub>2</sub>O + O<sub>2</sub> from 254 to 382 K. *J. Phys. Chem.* **1988**, *92*, 1193–1200.
- (7) Schwab, J. J.; Brune, W. H.; Anderson, J. G. Kinetics and mechanism of the OH + HO<sub>2</sub> reaction. *J. Phys. Chem.* **1989**, *93*, 1030–1035.
- (8) DeMore, W. B. Rate constant and possible pressure dependence of the reaction OH + HO<sub>2</sub>. *J. Phys. Chem.* **1982**, *86*, 121–126.
- (9) Cox, R. A.; Burrows, J. P.; Wallington, T. J. Rate coefficient for the reaction OH + HO<sub>2</sub> = H<sub>2</sub>O + O<sub>2</sub> at 1 atm pressure and 308 K. *Chem. Phys. Lett.* **1981**, *84*, 217–221.
- (10) Wine, P. H.; Semmes, D. H.; Ravishankara, A. R. A laser flash photolysis kinetics study of the reaction OH+H<sub>2</sub>O<sub>2</sub>→HO<sub>2</sub>+H<sub>2</sub>O. *J. Chem. Phys.* **1981**, *75*, 4390–4395.
- (11) Chang, J. S.; Kaufman, F. Upper bound and probable value of the rate constant of the reaction OH + HO<sub>2</sub> → H<sub>2</sub>O + O<sub>2</sub>. *J. Phys. Chem.* **1978**, *82*, 1683–1687.
- (12) Assaf, E.; Fittschen, C. Cross Section of OH Radical Overtone Transition near 7028 cm<sup>-1</sup> and Measurement of the Rate Constant of the Reaction of OH with HO<sub>2</sub> Radicals. *J. Phys. Chem. A* **2016**, *120*, 7051–7059.
- (13) Speak, T. H.; Blitz, M. A.; Medeiros, D. J.; Seakins, P. W. New Measurements and Calculations on the Kinetics of a Old Reaction: OH + HO<sub>2</sub> → H<sub>2</sub>O + O<sub>2</sub>. *JACS Au* **2023**, *3*, 1684–1694.
- (14) Chen, I.-Y.; Chang, C.-W.; Fittschen, C.; Luo, P.-L. Accurate Kinetic Studies of OH + HO<sub>2</sub> Radical–Radical Reaction through Direct Measurement of Precursor and Radical Concentrations with High-Resolution Time-Resolved Dual-Comb Spectroscopy. *J. Phys. Chem. Lett.* **2024**, *15*, 3733–3739.
- (15) Jenkins, J. M.; Brune, W. H.; Miller, D. O. Electrical Discharges Produce Prodigious Amounts of Hydroxyl and Hydroperoxyl Radicals. *J. Geophys. Res.: Atmos.* **2021**, *126* (9), No. e2021JD034557.
- (16) Rowe, J. P.; Lambe, A. T.; Brune, W. H. Technical Note: Effect of varying the λ = 185 and 254 nm photon flux ratio on radical generation in oxidation flow reactors. *Atmos. Chem. Phys.* **2020**, *20* (21), 13417–13424.
- (17) Faloon, I. C.; Tan, D.; Leshner, R. L.; Hazen, N. L.; Frame, C. L.; Simpas, J. B.; Harder, H.; Martinez, M.; Di Carlo, P.; Ren, X. R.; Brune, W. H. A laser-induced fluorescence instrument for detecting tropospheric OH and HO: Characteristics and calibration. *J. Atmos. Chem.* **2004**, *47* (2), 139–167.
- (18) Zhang, Z.; Padmaja, S.; Saini, R. D.; Huie, R. E.; Kurylo, M. J. Reactions of Hydroxyl Radicals with Several Hydrofluorocarbons: The Temperature Dependencies of the Rate Constants for CHF<sub>2</sub>CF<sub>2</sub>CH<sub>2</sub>F (HFC-245ca), CF<sub>3</sub>CHFCHF<sub>2</sub> (HFC-236ea), CF<sub>3</sub>CHFCF<sub>3</sub> (HFC-227ea), and CF<sub>3</sub>CH<sub>2</sub>CH<sub>2</sub>CF<sub>3</sub> (HFC-356ffa). *J. Phys. Chem.* **1994**, *98*, 4312–4315.
- (19) Saunders, S. M.; Jenkin, M. E.; Derwent, R. G.; Pilling, M. J. Protocol for the development of the Master Chemical Mechanism, MCM v3 (Part A): tropospheric degradation of nonaromatic volatile organic compounds. *Atmos. Chem. Phys.* **2003**, *3*, 161–180.
- (20) Wolfe, G. M.; Marvin, M. R.; Roberts, S. J.; Travis, K. R.; Liao, J. The Framework for 0-D Atmospheric Modeling (F0AM) v3.1. *Geosci. Model Dev.* **2016**, *9*, 3309–3319.